



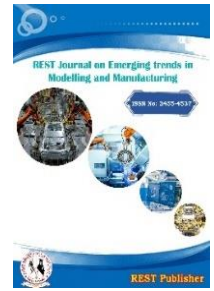
REST Journal on Emerging trends in Modelling and Manufacturing

Vol: 11(1), March 2025

REST Publisher; ISSN: 2455-4537 (Online)

Website: <https://restpublisher.com/journals/jemm/>

DOI: <https://doi.org/10.46632/jemm/11/1/3>



Hybrid Energy Management with Multiport DC-AC Inverter for Renewable Integration

* C.G. Revathi, T.MD. Jaffar Hussain, G. Sreenath, A. Anusha, N. Ramesh Kumar, A. Sadaq Khan

Annamacharya Institute of Technology & Sciences (Autonomous) Kadapa, Andhra Pradesh, India.

**Corresponding Author Email: revathireddy234.cg@gmail.com*

Abstract: This paper presents a novel non isolated multiport DC-AC inverter designed for distributed renewable energy systems integrated with hybrid energy storage solutions. The proposed inverter features a simplified architecture, utilising fewer passive components and high-frequency power semiconductors compared to conventional designs. The multiport converter (MPC) enables the integrated management of power from a photovoltaic (PV) array, battery unit, as upper capacitor bank, and an electric vehicle (EV) battery while supporting bidirectional power flow. The inverter's power circuit is based on an advanced split-source inverter topology, directly connecting the PV source to the DC link. A custom control method is developed for the MPC, allowing for maximum power point tracking (MPPT) of the PV array without additional converters, as well as independent regulation of power flow at each port and between the ports. The proposed control scheme ensures optimal energy utilization and enhances the system's flexibility while maintaining grid stability through ancillary services. Simulation validation of the various power flow scenarios demonstrates the effectiveness and robustness of the design. The results show improved efficiency and simplified system architecture, marking a significant step towards more cost-effective and scalable renewable energy systems.

1. INTRODUCTION

The global transition toward clean and sustainable energy has intensified in recent years, driven by the need to mitigate climate change, reduce carbon emissions, and secure energy independence. Distributed renewable energy systems, including solar photovoltaic (PV) power, wind energy, and small-scale hydroelectric systems, have emerged as vital components in modern energy grids. These systems enable energy generation closer to the point of consumption, reducing transmission losses, increasing system resilience, and promoting energy security. Among these renewable sources, solar energy has seen rapid adoption due to its abundant availability, scalability, and decreasing cost of technology. Solar photovoltaic (PV) systems are being increasingly integrated into residential, commercial, and industrial power networks. Despite the numerous advantages of renewable energy systems, challenges remain in efficiently managing and integrating these sources into existing electrical grids. The intermittent and variable nature of renewable energy sources like solar power means that energy generation is often inconsistent, depending on environmental conditions such as sunlight and weather. This variability, combined with growing demand for energy storage solutions, creates an intricate set of requirements for the design of power electronics systems that can effectively integrate, manage, and distribute energy. The integration of hybrid energy storage systems, such as batteries, super capacitors, and electric vehicle (EV) batteries, with renewable energy sources adds another layer of complexity. These storage technologies have unique characteristics such as charge/discharge rates, efficiency, and power density that necessitate sophisticated power conversion and management techniques to ensure optimal energy utilization. Power inverters play a critical role in modern distributed energy systems, acting as the interface between the energy sources (e.g., PV arrays, batteries) and the electrical grid or local loads. Inverters convert the DC output of the energy sources into AC power suitable for grid synchronization and local consumption. Conventional inverters typically use separate conversion units for each energy source, which increases the complexity and cost of the overall system. As the number of connected energy sources and storage elements increases, traditional designs often suffer from inefficiency, larger form factors, and higher component costs due to the need for additional converters and passive components. Moreover, the bi-directional flow of power in hybrid energy storage systems, where energy can be both supplied to and drawn from storage devices, further complicates the inverter design. In this context, the development of a non isolated multiport DC-AC inverter represents a novel solution that addresses the challenges of system complexity, efficiency, and

cost-effectiveness. A multiport converter (MPC) offers a significant improvement over traditional designs by integrating multiple power sources and storage systems in a single, unified converter structure. The proposed inverter is designed to handle power from arrange of sources, including PV array, a battery unit, as upper capacitor bank, and an EV battery, while simultaneously supporting bidirectional power flow. By reducing the number of required converters and passive

components, the system’s overall size and cost are significantly reduced, leading to more compact, scalable, and cost-effective renewable energy solutions.

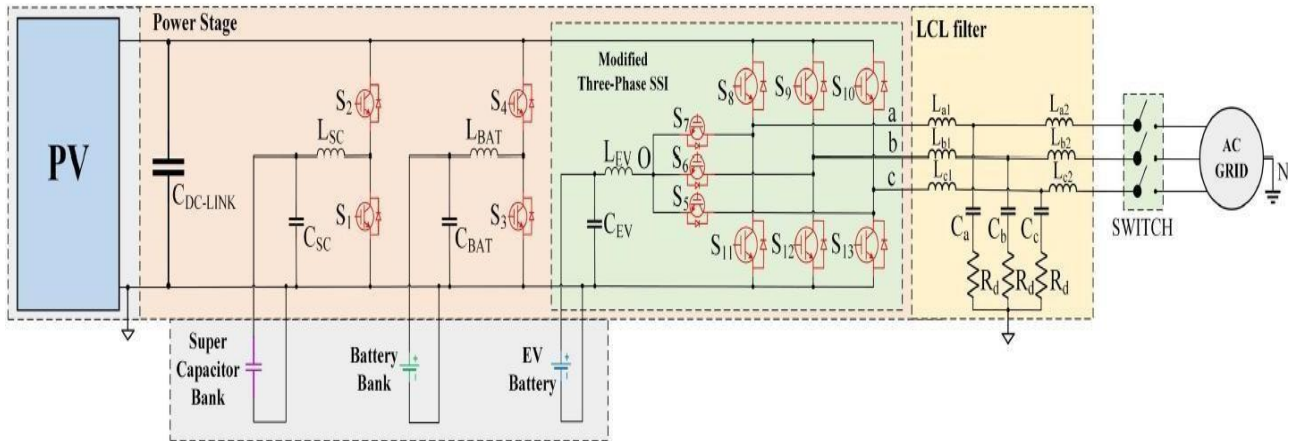


FIGURE 1. Circuit diagram of the proposed three-phase MPC inverter

Power circuit structure: As shown in Fig. 1, the proposed MPC inverter features four DC ports and one AC port. The DC ports are used for the interconnection of the PV array, SC, battery banks, and EV battery. The AC side can be connected to an AC load or grid. The PV array is connected directly to the DC-link capacitor ($C_{DC-link}$). The DC-link voltage is continuously modified by the control unit of the proposed MPC inverter in order to perform the MPPT process, as analyzed in the following. The battery and SC are connected to the DC link via bidirectional power circuits. Since the DC-link voltage is continuously regulated by the MPPT process, appropriate control of the battery and SC interconnection circuits has been developed, as also described next, in order to coordinate the power flow among the different input/output ports of the proposed MPC inverter. Each of these subcircuits receives as input the corresponding source in order to accomplish a two-way current flow by using two insulated-gate bipolar transistor (IGBT) power switches with antiparallel diodes. In [18], a single-phase version of SSI has been presented, where an inductor and a DC-link capacitor are integrated into a full-bridge inverter through two power switches. In this article, the work of Lee and Heng [18] is extended to a three-phase SSI, where the EV port inductor (L_{EV}) is connected to the switching nodes of a three-phase full-bridge inverter via three IGBT power switches (i.e., S_5, S_6 , and S_7 in Fig. 2) that operate at fundamental frequency. In contrast, if a separate DC–DC converter was used to interconnect the EV to the DC link, then power switches of high switching frequency would be required, thus increasing the cost and switching losses of the overall MPC inverter. In order to achieve the aforementioned functionality of the proposed MPC inverter power circuit, a special control method has also been developed in this article. One of the three legs of the full-bridge inverter should operate with a constant duty cycle for DC–DC conversion. The other two legs operate at a modified sinusoidal duty cycle for DC–AC output voltage production, as analyzed in the following. The three switches (S_5, S_6 , and S_7) that operate at fundamental frequency affect the DC-link voltage by clamping the leg that operates with a constant duty cycle to the inductor and EV battery port. As a result, the power flow can be regulated between the different ports of the proposed MPC inverter and, at the same time, in each port independently. The basic operational principle and the control strategies of the power switches are discussed next.

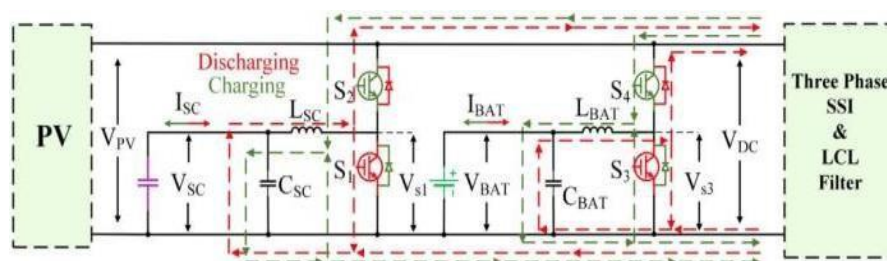
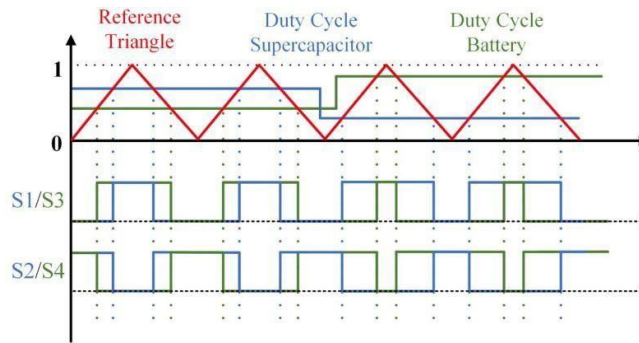


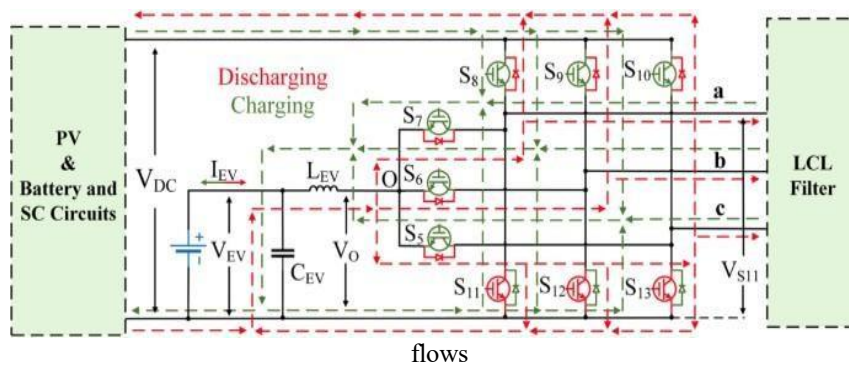
FIGURE 2. (a) Alternative current flow soft he battery and SC inter connection circuits of the proposed MPC inverter during a switching period

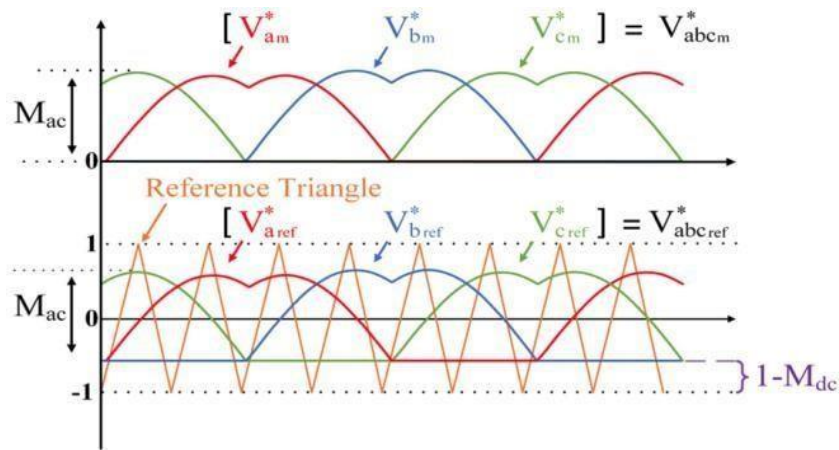


(b) Gate pulses for S1–S4

Principle of operation and driving signals: Based on the power balance among the ports of the proposed MPC inverter, multiple alternative power flow scenarios can be supported, as indicated with arrows in Fig. 1(b). The alternative current flows during the battery and SC charging and discharging modes during a switching period are shown in Fig. 3(a). The operational waveforms and gate signals of S1–S4 are illustrated in Fig. 3(b). A constant (duty cycle) for each input source is compared with a triangular signal (reference triangle) with frequency equal to the desired switching frequency of the MPC inverter. As long as the duty cycle is greater than the value of the triangle pulse, then the switch is set in the OFF-state, otherwise is ON. The switches S1 and S3 operate complementary to S2 and S4, respectively. The three-phase bridge consists of three legs, one for each phase of the ac grid (a, b, c). Each leg of the bridge includes two IGBT switch with antiparallel diodes, which receive complementary pulses. Therefore, S8 is complementary to S11 for phase a, S9 to S12 for phase b, and S10 to S13 for phase c, respectively. The EV battery is connected in series with LEV, which charges and discharges in appropriate cycles regulated by the control of the power switches. The inductor LEV is linked to three IGBTs with anti-parallel diodes (S7, S6, and S5), each connected to one leg (a, b, c) of the full-bridge circuit. As a result of this connection, there is an interaction between the control of the three-phase bridge circuit and the EV battery, which is further analyzed in the following. In Fig. 3(a), the alternative current flows of the modified three-phase SSI sub circuit of the proposed MPC inverter (see Fig. 1) with the EV source are displayed. In order to produce appropriate driving pulses for the IGBTs of the full-bridge circuit and the EV battery, three symmetrical sinusoidal reference waves with a phase difference of 120° are initially produced in the control unit of the proposed MPC inverter. Then, the three sinusoidal waves are modified as described in Section III, producing the reference signals, as illustrated in Fig. 3(b). The ac modulation index M_{ac} represents the amplitude of the reference signal and the dc modulation index M_{dc} corresponds to the offset of the reference signal. The values of M_{ac} and M_{dc} are adjusted in such a way as to achieve the desired power flow. To generate the driving pulses of S7, S6, and S5, the reference signal from the AV is measured against zero. The reference signal from the power switch is equal to zero, then the corresponding switch is set ON; otherwise, it is set OFF. This procedure is presented in Fig. 4(a). In order to generate the driving pulses for the three-phase bridge switches, while the reference signal for each leg of the full bridge is greater or equal to the width of the triangle pulse, then the corresponding switch is set ON; otherwise, it is set OFF [see Fig. 4(b)]. Switches S8, S9, and S10 are complementary to S11, S12, and S13, respectively.

FIGURE 3. Operation of the modified three-phase SSI sub circuit of the proposed MPC inverter. (a) Alternative current





(b) Reference signals

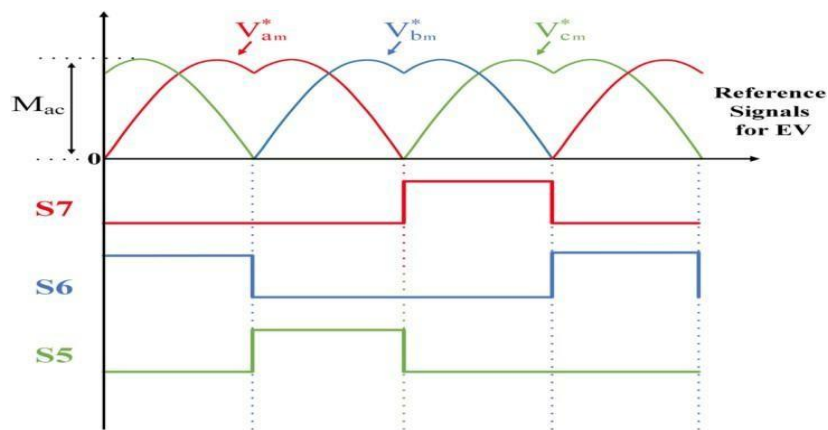


FIGURE 4. Gate pulses for (a) EV port switches and

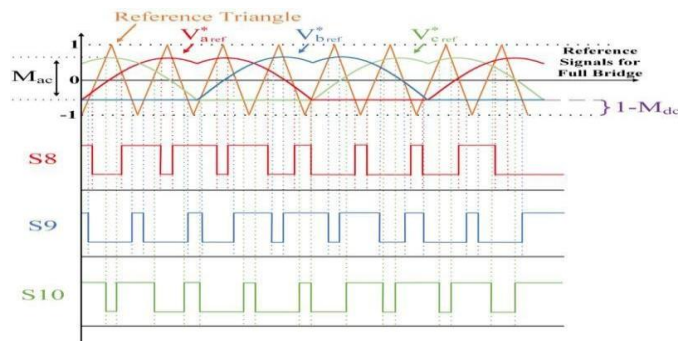


FIGURE 4. Gate pulses for (b) Full-bridge switches

As mentioned before, the reference signals for the control of the three EV switches have a phase difference of 120° . Hence, at every 120° (charging cycle), a different switch is set OFF. In every charging cycle, one leg of the bridge is acting as dc–dc converter for the dc-link voltage and the other two are responsible for the dc–ac conversion. For instance, as it is shown in Fig. 5(a), when S7 is ON and S6 and S5 are OFF, then the leg of the three-phase bridge that S7 is connected to operates as ac–dc converter and the other two legs control the dc–ac inversion. The same procedure is followed for the remaining two

power switches. In this way, the EV port of the SSI sub circuit is charging with a constant current, which is received from the three different power switches of the EV port (see Fig. 5).

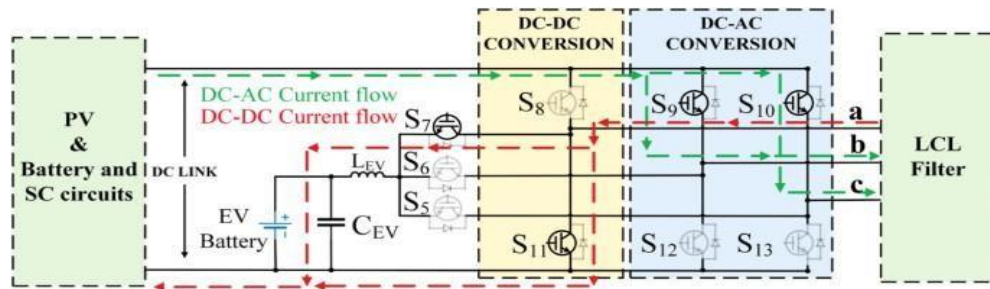
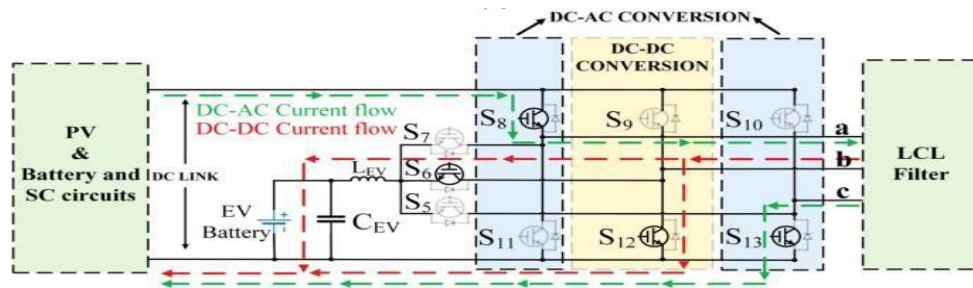
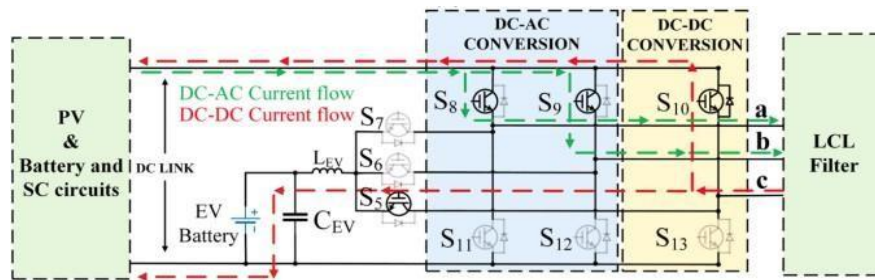


FIGURE 5: Alternative switching states of the modified three-phase SSI sub circuit of the proposed MPC inverter during charging. (a) State 5



(b) State 9



(c) State 24

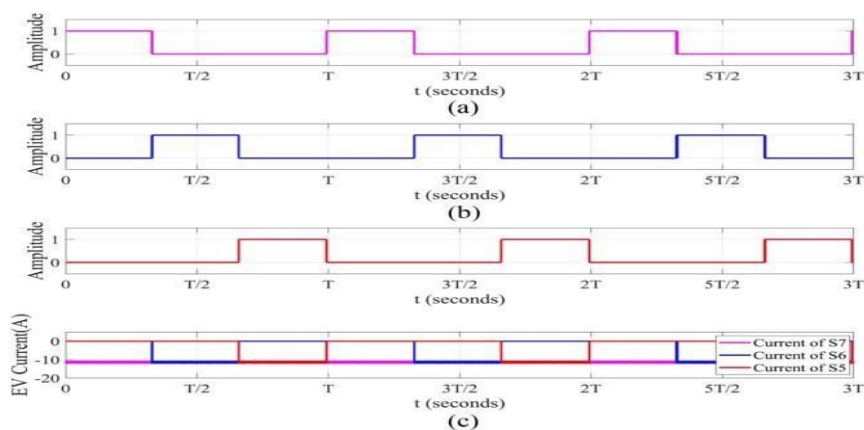


FIGURE 6: Gate pulses on (a) S7, (b) S6, (c) S5, and (d)EV battery current.

Table II lists all possible switching state combinations of the SSI sub circuit, where “1” and “0” represent the ON and OFF states of the associated switch. The connection of the SSI port indicates that the EV battery switches (S7, S6, and S5) should also be considered. The activation of only one of the three switches in each cycle allows for three potential states (100, 010, and 001). These three states can be combined with each of the eight states of the full bridge, for a total of 24 states. However, as indicated in Table II, only 15 of these states are valid, while the remaining 9 states are not feasible. In order for the EV switch connected to a full-bridge leg to be turned ON, the reference signal for that leg must be equal to $1 - M_{dc1} - M_{dc}$. As shown in Fig. 4, when the reference triangle is greater than $1 - M_{dc1} - M_{dc}$ and lower than the modulating signals ($V_{abc,ref} * V_{abc,ref}^*$) maximum value, the high-side switch of the leg that is operating at a constant duty cycle is OFF. The switch of that leg is ON only when the reference triangle is less than $1 - M_{dc1} - M_{dc}$. In such a case, the other two high-side switches are also turned ON because the values of their modulating signals are greater than the reference triangle. This means that the only way a high-side switch operating at a constant duty cycle is ON (i.e., the corresponding EV switch is ON) is when the other two high-side switches are also ON. The states 4–21 represent the region between $1 - M_{dc1} - M_{dc}$ and the modulating signals' maximum value. As a result, the states where a high-side switch of one phase is turned ON simultaneously with the corresponding EV switch are not valid.

TABLE 1: Switching states of the SSI sub circuit

State #	S ₈	S ₉	S ₁₀	S ₇	S ₆	S ₅	Valid
1	0	0	0	1	0	0	✓
2	0	0	0	0	1	0	✓
3	0	0	0	0	0	1	✓
4	1	0	0	1	0	0	X
5	1	0	0	0	1	0	✓
6	1	0	0	0	0	1	✓
7	1	1	0	1	0	0	X
8	1	1	0	0	1	0	X
9	1	1	0	0	0	1	✓
10	0	1	0	1	0	0	✓
11	0	1	0	0	1	0	X
12	0	1	0	0	0	1	✓
13	0	1	1	1	0	0	✓
14	0	1	1	0	1	0	X
15	0	1	1	0	0	1	X
16	0	0	1	1	0	0	✓
17	0	0	1	0	1	0	✓
18	0	0	1	0	0	1	X
19	1	0	1	1	0	0	X
20	1	0	1	0	1	0	✓
21	1	0	1	0	0	1	X
22	1	1	1	1	0	0	✓
23	1	1	1	0	1	0	✓
24	1	1	1	0	0	1	✓

The 15 remaining switching states, as shown in Table I, can occur in either the charging or discharging process of the EV battery. The discharging process is detailed in [16], while the equivalent circuit diagram of the modified three-phase SSI subcircuit (see Fig. 1) during the charging process of the EV port is presented in Fig. 5. In particular, states 5, 9, and 24 in Table II, which represent the current flow in all three switching states of the EV port switches S7, S6, and S5, are illustrated in Fig. 5.

Model Predictive Control (MPC): In the context of multiport DC–AC inverters integrated with hybrid renewable energy storage systems, Model Predictive Control (MPC) can help achieve efficient energy management, improve grid stability, and optimize power distribution across multiple energy sources, such as photovoltaic (PV) arrays, batteries, super capacitors, and electric vehicle (EV) batteries. Given the growing interest in renewable energy systems, particularly in off-grid and micro grid applications, MPC's ability to manage multiple power flows and ensure optimal performance has garnered significant attention.

2. SYSTEM MODELLING FOR MULTIPOINT DC–AC INVERTERS

For MPC to function effectively, an accurate system model is required. In the case of multiport DC–AC inverters, the model must describe the relationship between various energy sources, storage systems, and the grid or load. These systems typically involve multiple dynamic components, each with its own behavior, but the inverter and energy storage systems are the primary focus.

State-Space Model: A state-space model is commonly used to describe the dynamic behavior of systems, as it allows the system's evolution to be predicted overtime. Let the system state vector be denoted as $x(k)$, which encapsulates the system's state variables, including the voltages, currents, and states of charge (SOC) of storage devices. The control inputs $u(k)$ are the control signals that the MPC adjusts.

For a discrete-time system, the relationship between the system's state at time step k and at the next time step $k+1$ can be

$$x(k + 1) = Ax(k) + Bu(k)$$

expressed as:

where:

- $x(k) \in \mathbb{R}^n$ is the state vector at time k ,
- $u(k) \in \mathbb{R}^m$ is the control input vector at time k ,
- $A \in \mathbb{R}^n \times n$ is the state transition matrix,
- $B \in \mathbb{R}^n \times m$ is the input matrix.

The output $y(k)$, which could represent quantities like power or voltage, is related to the state by:

$$y(k) = Cx(k)$$

where $C \in \mathbb{R}^p \times n$ is the output matrix. This model forms the basis for prediction in MPC, where the future system states are predicted based on the current state and control inputs.

Dynamics of Multiport DC–AC Inverters : In multiport DC–AC inverters, each port corresponds to an energy source (such as a PV array, battery, super capacitor, or EV battery). The system dynamics are governed by the inter actions between these sources and the inverter, as well as the load or grid. Each port of the inverter can be described by a set of differential equations that represent the power flow and voltage/current relationships. The inverter’s switching dynamics are typically captured by modeling the equivalent circuits of each port and considering the power flow between the ports and the grid. For example, a simplified model for a PV array connected to an inverter can be expressed as:

$$P_{PV} = V_{PV} \cdot I_{PV}$$

where P_{PV} is the power generated by the PV array, V_{PV} is the voltage at the PV terminals, and I_{PV} is the current supplied by the PV array.

Similarly, for a battery storage system, the dynamics could be represented as:

$$P_{battery} = V_{battery} \cdot I_{battery} \quad \text{and} \quad SOC(k+1) = SOC(k) + \Delta SOC$$

where $P_{battery}$ is the power drawn from or supplied to the battery, $V_{battery}$ is the battery voltage, and $I_{battery}$ is the battery current. The SOC (state of charge) of the battery changes based on the charging or discharging current, and it is constrained within certain bounds to ensure the battery’s health.

The total power balance of the system is governed by the interaction of all these components and can be expressed as:

$$P_{total} = P_{PV} + P_{battery} + P_{supercapacitor} + P_{EV} - P_{load}$$

where P_{total} is the total power supplied to the grid or local load, and P_{load} is the demand from the load.

Cost Function in MPC

The cost function plays a central role in MPC as it defines the objective of the optimization problem. In power systems, the goal is often to minimize energy losses, maintain system stability, and ensure that power generation matches consumption.

For a multiport inverter system, the cost function can be structured as follows:

$$J = \sum_{i=0}^{N-1} ((y(k+i) - r(k+i))^T Q (y(k+i) - r(k+i)) + (u(k+i))^T R u(k+i))$$

where:

- $Y(k+i)$ is the predicted output (e.g., power or voltage) at time step $k+i$,
- $R(k+i)$ is the reference trajectory (desired power or voltage) at time step $k+i$,
- $Q \in \mathbb{R}^p \times p$ and $R \in \mathbb{R}^m \times m$ are positive definite weighting matrices that penalize deviations in outputs and large control inputs, respectively.

The first term $(y(k+i) - r(k+i))^T Q (y(k+i) - r(k+i))$ penalizes the deviation between the system’s output and the reference, ensuring that the system follows the desired power profile. The second term $(u(k+i))^T R u(k+i)$ Penalizing large control inputs helps promote energy-efficient operation and reduces wear on components. This can be achieved by adding a term to the cost function that penalizes excessive control effort. The modified cost function can be expressed as:

Constraints in MPC: One of the key strengths of MPC is its ability to handle constraints on system behavior. In the context of multiport DC–AC inverters, several physical, operational, and safety constraints must be considered:

Energy Storage Constraints: The state of charge (SOC) of batteries or super capacitors should remain within a certain range to avoid overcharging or deep discharging, which can lead to performance degradation or failure.

$$SOC_{\min} \leq SOC(k + i) \leq SOC_{\max}$$

Voltage and Current Limits: The inverter and energy storage devices have maximum and minimum voltage and current limits that must be respected.

$$V_{\min} \leq V(k + i) \leq V_{\max}, \quad I_{\min} \leq I(k + i) \leq I_{\max}$$

Power Flow Constraints: The total power flow to the grid or load must not exceed a specified capacity. This constraint can be expressed as:

$$P_{\text{total}}(k + i) \leq P_{\max}$$

Operational Constraints: The system may have additional operational constraints, such as thermal limits, limits for the inverter or safety margins for power electronics.

Optimization Problem Formulation

The optimization problem for MPC is formulated as:

$$\min_{u(k), \dots, u(k+N-1)} J(u(k), \dots, u(k + N - 1), x(k))$$

Subject to:

$$x(k + 1) = Ax(k) + Bu(k)$$

$$y(k + i) = Cx(k + i)$$

$$u_{\min} \leq u(k + i) \leq u_{\max}, \quad x_{\min} \leq x(k + i) \leq x_{\max}$$

$$SOC_{\min} \leq SOC(k + i) \leq SOC_{\max}$$

The objective is to minimize the cost function J while satisfying the system dynamics and constraints. The optimization problem is solved at each time step, and the first control input from the optimal sequence is applied to the system.

Numerical Solution and Computational Techniques: The optimization problem in MPC is typically solved using numerical optimization techniques, such as:

- **Quadratic Programming (QP):** Used for problems with quadratic cost functions and linear constraints, such as in many power system applications.
- **Nonlinear Programming (NLP):** For more complex problems where the system dynamics or constraints are nonlinear. To implement MPC in real time, efficient solvers with low computational overhead are essential. The complexity of solving the optimization problem grows with the prediction horizon, the number of system states, and the number of control inputs. Therefore, approximations and efficient algorithms, such as gradient-based methods or fast MPC solvers, are used to ensure real-time applicability.

Model Predictive Control (MPC) offers a powerful tool for managing multiport DC–AC inverters in hybrid renewable energy systems. Its ability to predict future system behavior, optimize control actions, and respect system constraints makes it ideal for ensuring efficient energy management in complex systems with multiple power sources, storage devices, and energy flows. By solving an optimization problem, at each time step, MPC ensures that renewable energy systems operate efficiently while maintaining stability.

3. RESULTS

A MATLAB Simulink of the proposed MPC inverter has been developed and tested in order to validate the operation of both the power circuit and associated control scheme. An SC bank and a battery were connected to the corresponding input ports, while another battery has been connected at The EV port of the proposed MPC inverter. The PV array was connected directly to the dc link according to the proposed topology, as shown in Fig. 2. The output of the power circuit of the proposed MPC inverter was finally Connected via an LCL-type output filter to a three-phase isolation step-up transformer. (Turns ratio 1:18) for protection purposes and then to the AC electric grid. These results verify the successful operation of both the power circuit and the control scheme implemented in the DSP controller of the proposed MPC inverter. To further evaluate the performance of the proposed MPC inverter, various experimental power flow scenarios were carried out. The corresponding results are presented in Fig. 7. It is observed that the PV power has a constant value in every state of operation as obtained by the execution of the PV MPPT algorithm. Furthermore, the power levels of the battery, EV port, and SC bank are varying and follow successfully the corresponding power set point of each state.

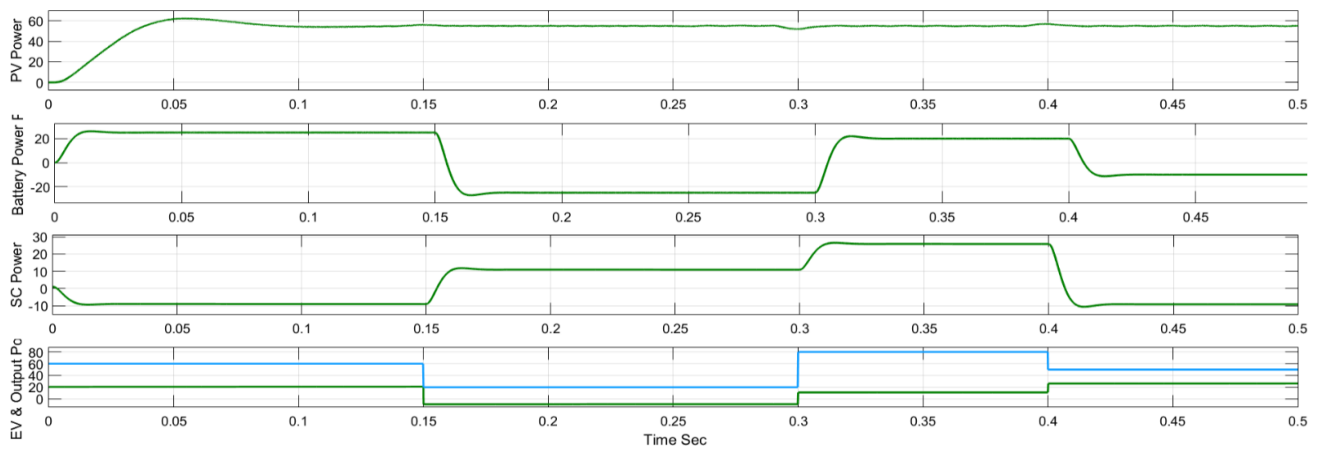


FIGURE 7. Simulation measured power flows during different operational

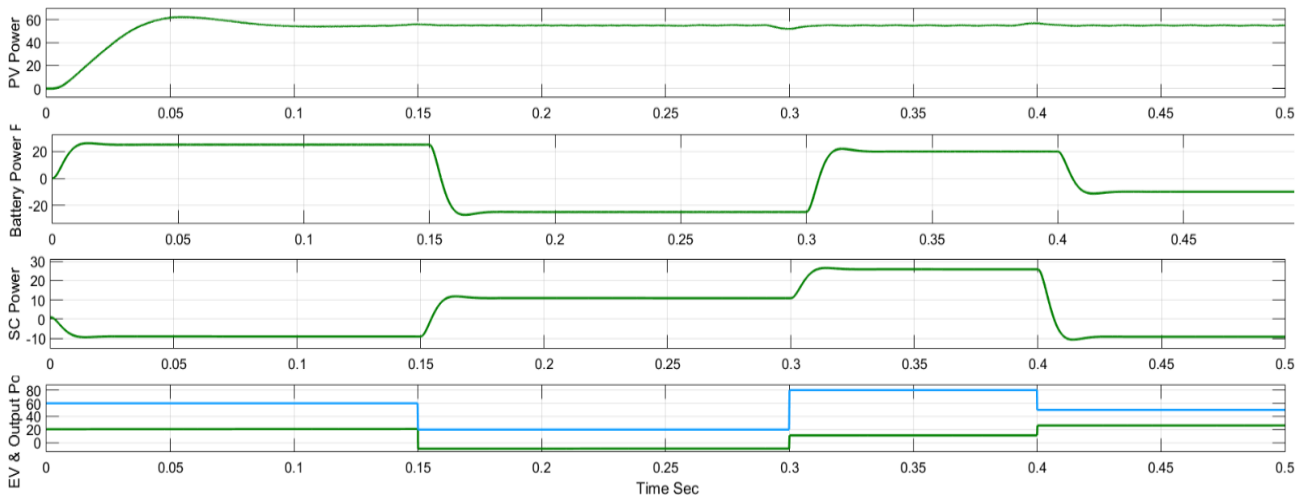


FIGURE 8. Simulation measured power flows and MPPT operation during partial shading conditions

The ability of the proposed MPC inverter to independently perform the MPPT process was experimentally verified under PV array partial shading conditions, as depicted in Fig. 19. The power flows of the battery bank, EV port, and SC were intentionally set to vary by the DSP-based control unit of the MPC inverter. It is observed that despite the variations of the MPP power and dc-link voltage due to the change of the incident solar irradiance, the proposed MPC inverter successfully tracked the MPPs of the PV source and simultaneously achieved to regulate independently the power flow of the battery, EV, and SC ports, respectively, at the desired levels.

4. CONCLUSION

The integration of distributed renewable energy systems, particularly solar PV, into modern power grids presents significant opportunities to reduce carbon emissions and enhance energy security. However, the intermittent nature of these energy sources, combined with the growing need for efficient energy storage solutions, introduces substantial challenges in terms of grid stability and power management. The development of non-isolated multiport DC–AC inverters offers a promising solution to address these challenges by consolidating multiple power sources and storage systems into a single, unified converter architecture. The proposed multiport converter improves system efficiency, reduces complexity, and lowers costs by minimizing the number of required converters and passive components. Additionally, its support for bidirectional power flow makes it ideal for managing energy storage systems, such as batteries, super capacitors, and electric vehicle (EV) batteries, in hybrid configurations. The reduction in system size and cost makes it a scalable and cost-effective solution, enhancing the overall viability of renewable energy systems for residential, commercial, and industrial applications. Future research and development efforts should focus on optimizing the control strategies and enhancing the performance of multiport converters in the face of varying grid conditions and load demands. Furthermore, integration with emerging smart grid technologies could further improve the efficiency and reliability of hybrid renewable energy systems. Continued advancement of power electronics, coupled with the growing adoption of renewable energy sources, will play a pivotal role in achieving global sustainability goals and ensuring a secure and resilient energy future.

REFERENCES

- [1]. t. Ariyaratna, n. Kularatna, k. Gunawardane, d. Jayananda, and d. A. Steyn-ross, “development of supercapacitor technology and its potential impact on new power converter techniques for renewable energy,” *ieec j. Emerg. Sel. Topics ind. Electron.*, vol. 2, no. 3, pp. 267–276, jul. 2021.
- [2]. d. G. A. Krishna, k. Anbalagan, k. K. Prabhakaran, and s. Kumar, “an efficient pseudo-derivative-feedback-based voltage controller for dvr under distorted grid conditions,” *ieec j. Emerg. Sel. Topics ind. Electron.*, vol. 2, no. 1, pp. 71– 81, jan. 2021.
- [3]. b.R.Ravada,n.R.Tummuru,andb.N.L.Ande,“agrid-connected converter configuration forthesynergy ofbattery- supercapacitor hybridstorageand renewable energy resources,” *ieec j. Emerg. Sel.Topicsind. Electron.*, vol.2,no.3,pp. 334–342, jul. 2021.
- [4]. s.Gao,h.Li,j.Jurasz,andr.Dai,“optimalchargingofelectricvehicleaggregationsparticipatinginenergyandancillary service markets,” *ieec j. Emerg. Sel. Topics ind. Electron.*, vol. 3, no. 2, pp. 270–278, apr. 2022.
- [5]. h. Heydari-doostabadandt. O’donnell, “awide-rangehigh-voltage-gainbidirectionaldc–dc converterforv2gandg2v hybrid ev charger,” *ieec trans. Ind. Electron.*, vol. 69, no. 5, pp. 4718–4729, may 2022.
- [6]. a. Balal and m. Giesselmann, “pv to vehicle, pv to grid, vehicle to grid, and grid to vehicle micro grid system using level three charging station,” in *proc. Ieee green technol. Conf.*, 2022, pp. 25–30.
- [7]. w. Jiang and b. Fahimi, “multiport power electronic interface—concept, modeling, and design,” *ieec trans. Power electron.*, vol. 26, no. 7, pp. 1890–1900, jul. 2011.
- [8]. p. Shamsi and b. Fahimi, “dynamic behavior of multiport power electronic interface under source/load disturbances,” *ieec trans. Ind. Electron.*, vol. 60, no. 10, pp. 4500–4511, oct. 2013.
- [9]. z. Ni, a. Abuelnaga, and m. Narimani, “a novel high-performance predictive control formulation for multilevel inverters,” *ieec trans. Power electron.*, vol. 35, no. 11, pp. 11533–11543, nov. 2020.
- [10]. j.Zeng,j.Ning,x.Du,t.Kim,z.Yang,andv.Winstead,“afour-portdc–dcconverterforastandalonewind andsolar energy system,” *ieec trans. Ind. Appl.*, vol. 56, no. 1, pp. 446–454, jan./feb. 2020.